M GIANT KINEMATICS IN OFF-AXIS FIELDS BETWEEN 150 AND 300 PC FROM THE GALACTIC CENTER

R. D. BLUM, J. S. CARR, K. SELLGREN AND D. M. TERNDRUP
The Ohio State University
174 W. 18th Ave., Columbus, Oh, 43210, USA

Abstract. We present radial velocities for approximately 40 stars in each of four optically obscured, off-axis fields toward the Galactic bulge. The mean heliocentric radial velocity and velocity dispersion are -75 ± 24 km s^{-1} and 127 ± 16 km s^{-1}, 2 ± 23 km s^{-1} and 127 ± 14 km s^{-1}, -14 ± 22 km s^{-1} and 126 ± 14 km s^{-1}, and -31 ± 28 km s^{-1} and 153 ± 17 km s^{-1} for fields located at 299, 288, 171, and 160 pc projected radius, respectively. The dispersions generally match Kent's (1992) axisymmetric mass model but may be higher than the model's predictions at small projected radius.

1. Introduction

Recent photometric studies have produced strong evidence that the inner Galaxy is barred (Blitz and Spergel 1991, Weiland et al. 1994, Stanek et al. 1994, and Dwek et al. 1994). In addition, dynamical modeling of observed gas kinematics also indicates that the inner Galaxy is non-axisymmetric (Binney et al. 1991). However, clear evidence for a non-axisymmetric potential has not been found in the observed stellar kinematics. Indeed, Kent's (1992) axisymmetric dynamical model of the Galactic bulge fits the available data well.

To better constrain the inner Galaxy mass distribution, we have obtained radial velocities for stars in each of four fields located at off-axis positions between 150 and 300 pc projected radius from the Galactic Center (GC). Kent's model predicts a change in the projected dispersion as a function of distance at these radii, but until now, no stellar kinematic data were available here. The large amount of extinction toward the GC at optical wavelengths requires spectroscopic observations at near infrared or

L. Blitz and P. Teuben (eds.), Unsolved Problems of the Milky Way, 111–117.
© 1996 *International Astronomical Union. Printed in the Netherlands.*

https://doi.org/10.1017/S0074180900229586 Published online by Cambridge University Press

longer wavelengths. We obtained the radial velocities using spectra centered near the 2.3 μm CO bandhead, a strong photospheric absorption feature in M giants.

The data for one of the fields shown here has been presented earlier by Blum et al. (1994).

2. Observations

The program stars were selected from the brighter and redder stars on K and J band images obtained with the Ohio State Infrared Imaging System (OSIRIS) on the Perkins 1.8m telescope near Flagstaff, Arizona during May 1992 and March 1993. OSIRIS employs a 256×256 NICMOS III array.

The majority of the spectroscopic observations were made on the CTIO 1.5m telescope in July 1992 and 1993 using the facility infrared spectrometer (IRS) which employs an SBRC 58×62 InSb detector. The spectral resolution was 84 km s^{-1} (42 km s^{-1} pix^{-1}) at the 2.3 μm CO bandhead. The velocities for stars in one field were obtained in July 1994 using the IRTF 3m infrared telescope and facility echelle spectrometer, CSHELL. The spectral resolution was 25 km s^{-1} (2.5 km s^{-1} pix^{-1}).

Figure 1 shows the spectra of a radial velocity standard and program star measured on each system. The uncertainty in an individual velocity is approximately $\pm$ 15 km s^{-1} as determined from the rms difference of measurements of 15 program stars on both systems.

3. Color Magnitude Diagram

The mean intrinsic $J - K$ can be estimated from the measured CO absorption strengths which are independent of reddening. The mean intrinsic $J - K$ can then be combined with the mean observed $J - K$ to derive the reddening for each field. Comparison of our mean CO strength with the disk M giant spectra in Kleinmann & Hall (1986) and the bulge giant spectra from Terndrup et al. (1991) suggests a mean spectral type of about M5-M7 III or later. This corresponds to an intrinsic $J-K$ of about 1.15 for the stars in Terndrup et al. (1990). The derived reddening given in Table 1 is based on the interstellar reddening curve of Mathis (1990).

The de-reddened color-magnitude diagram (CMD) for the program stars is shown in Figure 2. The left panel depicts the CMD for stars in the four fields for which $K \lesssim 9$. The right hand panel shows those stars for which we obtained spectra. The stars in Figure 2 were corrected for extinction as described above. The derived extinction at K is given for each field in Table 1. The photometric uncertainties in J and K are $\lesssim \pm$ 0.10 mag.

In Figure 2, we also show the unreddened mean and median color v. magnitude relations for the Baade's Window M giants measured by Frogel

https://doi.org/10.1017/S0074180900229586 Published online by Cambridge University Press

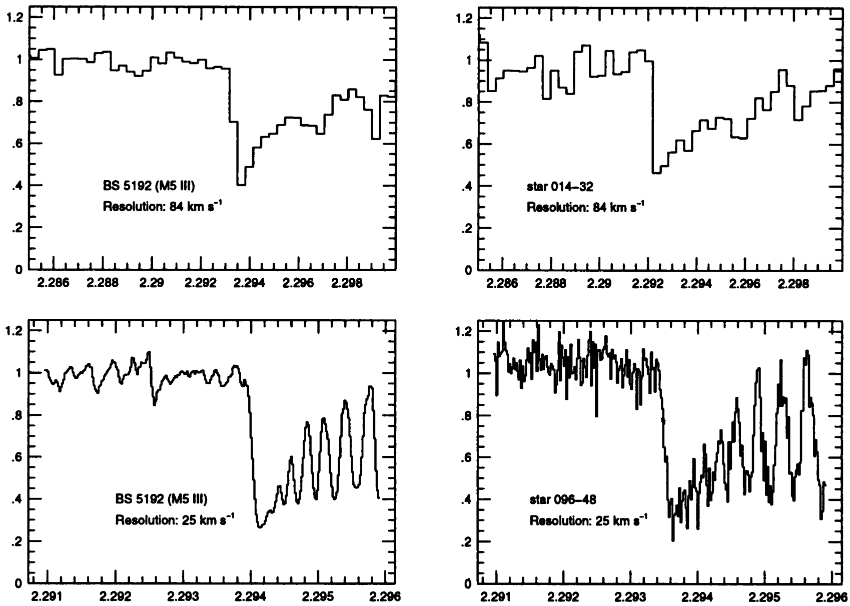

Figure 1. Upper panels, CTIO IRS spectra: resolution = 84 km s^{-1} (42 km s^{-1} pix^{-1}). Lower panels, IRTF CSHELL spectra: resolution = 25 km s^{-1} (2.5 km s^{-1} pix^{-1}). A typical radial velocity standard (BS 5192, M5 III) is shown along with two program stars.

& Whitford (1987). The majority of our stars lie near the Frogel & Whitford relations, suggesting they are also in the inner Galaxy.

4. Kinematics

The velocity dispersion and mean heliocentric radial velocity for each field is shown in Table 1. The distribution of velocities for each field is shown in Figure 3 along with the expected number from a Gaussian distribution of the same mean and dispersion. Kolmogorov-Smirnov (KS) tests show no statistical evidence that any of the observed distributions is different from Gaussian. However, because of the small number of stars in each field, we have not attempted to uniquely determine the form of the intrinsic distributions. There is no reason to expect *a priori* that the distribution of observed velocities should be Gaussian. Kuijken (1994) computed the distribution function for stars in the Kent (1992) isotropic oblate rotator model and found that the distribution in Baade's Window is well represented by a Gaussian. However, the predicted distribution of velocities for stars in another part of the bulge was not Gaussian.

https://doi.org/10.1017/S0074180900229586 Published online by Cambridge University Press

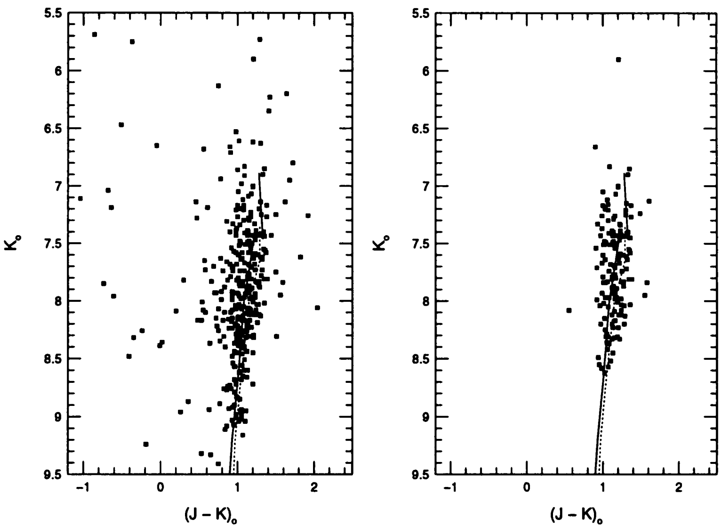

Figure 2. De-reddened color-magnitude diagram for the four program star fields. The extinction correction assumes the interstellar relation from Mathis (1990) and relies on using the observed CO strengths to determine the mean intrinsic color in each field. The left panel depicts the CMD for stars in the four fields for which observed $K \lesssim 9$. The right panel shows the stars for which we obtained spectra; their selection was based on color and magnitude. The lines are the mean (solid) and median (dashed) relations for Baade's Window taken from Frogel and Whitford (1987).

Table 1. M Giant Observed Properties

Field	l (deg)	b (deg)	R[a] (pc)	A_K[b]	v^c (km s^{-1})	σ (km s^{-1})
1	−0.59	0.98	160	0.99	−31 ± 28	153 ± 17
2	0.85	−0.88	171	0.74	2 ± 23	127 ± 14
3	1.21	−1.67	288	0.23	14 ± 22	126± 14
4	−1.14	1.81	299	0.59	−75 ± 24	127 ±17

Notes to Table 1: a) Assuming R_o = 8 kpc. b) Derived using the extinction law of Mathis (1990) and intrinsic color based on CO strength; see text. c) Mean heliocentric velocity.

A rough comparison to the observed kinematics can be made by comparing our projected velocity dispersions to Kent's prediction for the minor axis of the bulge (Figure 4). Three of our positions are consistent with Kent's model. The fourth position shows a dispersion which is larger than Kent's prediction (2 σ). The observed dispersion in Field 1 is possibly in-

https://doi.org/10.1017/S0074180900229586 Published online by Cambridge University Press

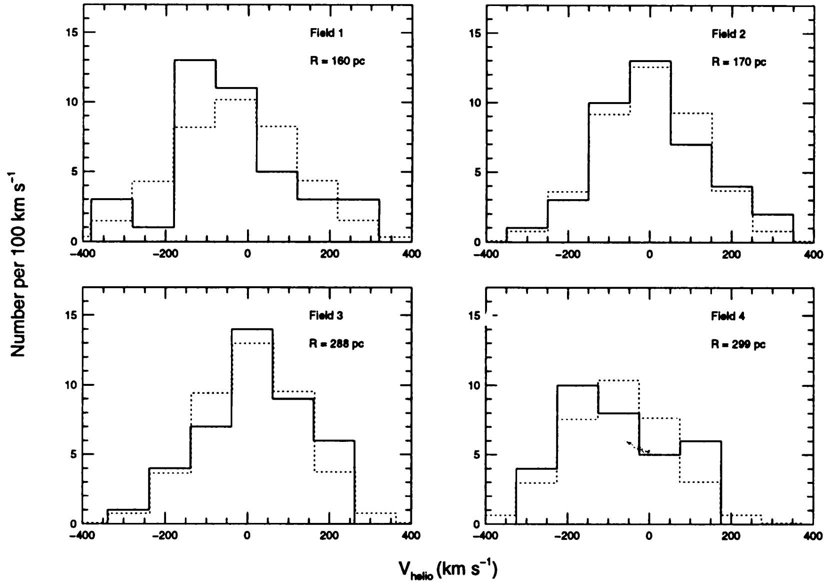

Figure 3. Observed heliocentric velocity distributions for each field (solid line). Distribution of velocities for a Gaussian of the observed FWHM and mean velocity (dashed line). Application of a Kolmogorov-Smirnov test shows no statistical evidence that the observed distributions are non-Gaussian.

consistent with a constant M/L ratio axisymmetric model since it would require a somewhat more peaked density distribution within about 100 pc. A more peaked density distribution with constant M/L is probably ruled out, however, by a preliminary comparison of recent COBE data (Dwek et al. 1994, Weiland et al. 1994) with the original Kent model (Kent, private communication). We note that the data shown in Figure 4 suggests that the line of sight dispersion may be constant or increasing at R $\lesssim$200 pc where Kent's model is decreasing.

A second possibility is that the higher line of sight dispersion in Field 1 results from a barred potential which we observe along a line of sight near its major axis. The dynamical model of Binney et al. (1991), derived from fitting the envelope of gas velocities in the l vs. v diagram, has a barred potential oriented with its major axis only 16° from our line of sight. Dwek et al. (1994) find a best fit triaxial model for the bulge by modeling the near infrared surface brightness distribution in the inner Galaxy. Their best fit model has its major axis oriented at 20° ± 10° to our line of sight. However, until realistic non-axisymmetric dynamical models that predict stellar kinematics are produced, no direct comparison can be made to the observations, and the mass distribution derived from stellar kinematics remains uncertain.

The mean velocities for three of the four fields are consistent with Kent's model. The velocity in field 4 is significantly more negative (2 σ) than

https://doi.org/10.1017/S0074180900229586 Published online by Cambridge University Press

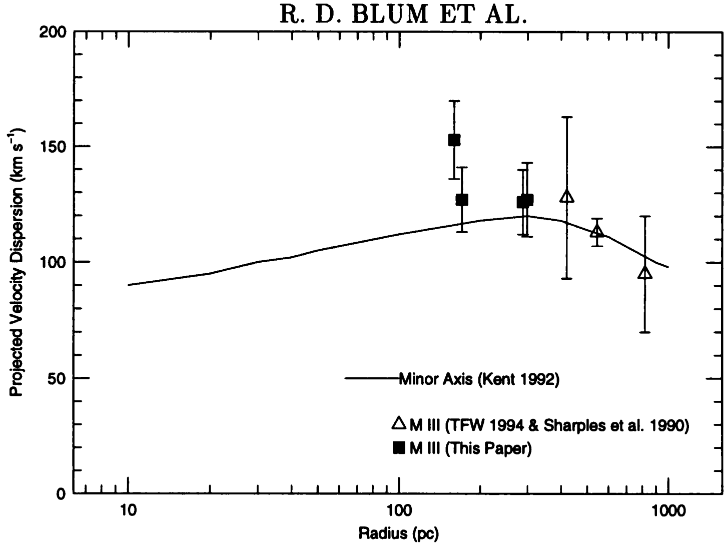

Figure 4. Comparison of observed and predicted line of sight velocity dispersions. The solid curve is taken from the oblate isotropic rotator model of Kent (1992).

predicted (-25 km s^{-1} for this line of sight, Kent, private communication). A gradient in mean velocity along the minor axis would be evidence for triaxiality. However, our fields lie along neither axis, so we can not easily separate the components of velocity along the two axes.

References

Binney, J., Gerhard, O. E., Stark, A. A., Bally, J., & Uchida, K.I., 1991, MNRAS, 252, 210
Blitz, L. & Spergel, D.N., 1991, ApJ, 379, 631
Blum, R. D., Carr, J. S,, DePoy, D. L., Sellgren, K., & Terndrup, D. M., 1994, ApJ, 422, 111
Dwek, E., et al., 1994, ApJ, submitted
Frogel, J. A. & Whitford, A.E., 1987, ApJ, 320, 199
Kent, S.M., 1992, ApJ, 387, 181
Kleinmann, S.G. & Hall, D.N.B., 1986, ApJS, 62, 501
Kuijken, K., 1994, preprint
Mathis, J.S., 1990, ARA&A, 28, 37
Sharples, R., Walker, A., & Cropper, M., 1990, MNRAS, 246, 54
Stanek, K. Z., Mateo, M., Udalski, A., Szymanski, M., Kaluzny, J. & Kubiak, M., ApJL, 429, L73
Terndrup, D.M., Frogel, J.A., & Whitford, A.E., 1991, ApJ, 378, 742
Terndrup, D.M., Frogel, J.A., & Whitford, A.E., 1990, ApJ, 357, 453
Terndrup, D. M, Frogel, J. A., & Wells, L., 1994, in preparation (TFW)
Weiland, J., et al., 1994, ApJL, 425, L81

https://doi.org/10.1017/S0074180900229586 Published online by Cambridge University Press

DISCUSSION

J. Sellwood: Some people may be surprised at how well Kent's axisymmetric model matches up to the kinematic data on the bulge which we believe to be triaxial. In order to fit the observations, an axisymmetric model must have kinematics intermediate between those on the major and minor axes. But we observe the bar at an intermediate angle, so intermediate kinematics should not be surprising.

Blum: No answer.

T. de Zeeuw: It is useful to compare not only the measured σ_{los} to Keitt's model but also the actual histogram of μ_{los}. Konrad Kuijken, e.g. has calculated expected distributions.

Blum: We would be happy to make comparisons between the observed velocity distribution and the predictions from Kuijken's analysis of the Kent model. We have already compared the observed distributions to gaussians of the observed width and mean velocity and find no significant statistical difference between them.

https://doi.org/10.1017/S0074180900229586 Published online by Cambridge University Press